A Molecular Rotor Based on an Unhindered Boron Dipyrromethene (Bodipy) Dye

Mohammed A. H. Alamiry, Andrew C. Benniston,* Graeme Copley, Kristopher J. Elliott, Anthony Harriman,* Beverly Stewart, and Yong-Gang Zhi

Molecular Photonics Laboratory, School of Natural Sciences, Newcastle University, Newcastle-upon-Tyne NE1 7RU, United Kingdom

Received March 10, 2008. Revised Manuscript Received April 10, 2008

This work describes a fluorescent probe for following changes in the viscosity of the surrounding medium. The optical properties, fluorescence characteristics, and sensitivity to frictional forces with the surrounding medium are superior to the most commonly used molecular probe, namely dicyanovinyl julolidine. The photophysical properties of the target molecule have been recorded in a range of solvents under ambient conditions, over a wide temperature range, and as a function of applied pressure. The mechanism by which the probe responds to changes in local viscosity involves gyration of the meso-phenylene ring and accompanying distortion of the dipyrrin framework, as indicated by molecular dynamics simulations. Indeed, temperature-dependence measurements have established that the activation energy is small when the solvent viscosity is relatively low, but there is a turnover to strong activation control at very high viscosity. A small but definite solvent dependence appears when the viscosity is varied by the application of high pressures and this can be traced to differences in the elasticity of the surroundings. Unusually for such fluorescent rotors, there is no indication that the excited state involves charge-transfer interactions. The rotor also responds to changes in the polarizability of the solvent, as induced by changes in applied pressure, and to the extent of polymerization of a monomer. The various experimental observations made at low viscosity are consistent with diffusive motion of the wave packet along the excited-state potential curve until finding a sink that strongly coupled to the highly distorted ground state.

Introduction

Local frictional forces exert a pronounced influence on the velocity at which a molecule might migrate through its environment. Consequently, there are many areas of chemistry, physics, and biology that require an in-depth understanding of the role that viscosity, both macroscopic and microscopic, plays in manipulating the dynamical properties of the solute. Perhaps the most noteworthy area is in chemical biology, where microscopic viscosity within cell membranes is important for controlling the movement of many critical species.[1] For example, the microviscosity of a cell membrane influences the activity of membrane-constrained proteins,[2] and any such alterations bring about modifications in physiological processes taking place within the cell.[3] These subtle changes have, in turn, been linked to various disease states including diabetes,[4] atherosclerosis,[5] and Alzheimer's disease.[6] It is not too surprising, therefore, that real-time detection of changes in viscosity in biological systems is a highly active research area.[7] Within the development field, fast response methods have tended to focus on the use of fluorescence,[8] especially because high spatial resolution is now readily attainable. Here, the techniques of fluorescence anisotropy[9] and fluorescence recovery after photobleaching[10] have dominated the field, although both suffer from limitations in time resolution and in the photostability of the probe molecule.

In an attempt to overcome some of these problems, recent developments of new fluorescence-based techniques have

* Telephone: 44 191 222 5706. Fax: 44 191 222 8660 . E-mail: a.c.benniston@ncl.ac.uk.

(1) Singer, S. J.; Nicolson, G. L. *Science* **1972**, *175*, 720–731.
(2) Shiga, T.; Maeda, N. *Biorheology* **1980**, *17*, 485–499.
(3) Akers, W. J.; Cupps, J. M.; Hiadekker, M. A. *Biorheology* **2005**, *42*, 335–344.
(4) Nadiv, O.; Shinitzky, M.; Manu, H.; Hecht, D.; Roberts Jr, C. T.; LeRoith, D.; Zick, Y. *Biochem. J.* **1994**, *298*, 443–450.
(5) Deliconstantinos, G.; Villotou, V.; Stavrides, J. C. *Biochem. Pharmacol.* **1995**, *49*, 1589–1600.
(6) Vanrensburg, S. J.; Daniels, W. M. U.; Vanzyl, J.; Potocnik, F. C. V.; Vnderwalt, B. J.; Tlajaard, J. J. F. *Neuroreport* **1994**, *5*, 2221–2224.
(7) Coelho Neto, J.; Agero, U.; Gazzinelli, R. T.; Mesquita, O. N. *Biophys. J.* **2006**, *91*, 1108–1115.
(8) (a) Haidekkar, M. A.; Brady, T. P.; Lichlyter, D.; Theodorakis, E. A. *J. Am. Chem. Soc.* **2006**, *128*, 398–399. (b) Fischer, D.; Theodorakis, E. A.; Haidekker, M. A. *Nat. Protoc.* **2007**, *2*, 227–236. (c) Bondarev, S. L.; Knyukshto, V. N.; Tikhomirov, S. A.; Maslov, N. V. *J. Appl. Spectrosc.* **2000**, *67*, 935–938. (d) Rosspeintner, A.; Kattnig, D. R.; Angulo, G.; Landgraf, S.; Grampp, G.; Cuetos, A. *Chem.—Eur. J.* **2007**, *13*, 6474–6483. (e) Luby-Phelps, K.; Mujumdar, S.; Mujumdar, R. B.; Ernst, L. A.; Galbraith, W.; Waggoner, A. S. *Biophys. J.* **1993**, *65*, 236–242.
(9) (a) Balter, A.; Szubiakowski, J. *J. Fluoresc.* **1993**, *3*, 247–249. (b) Dix, J. A.; Verkman, A. S. *Biophys. J.* **1990**, *57*, 231–240. (c) Binenbaum, Z.; Klyman, E.; Fishov, I. *Biochem.* **1999**, *81*, 921–929. (d) Foster, T. H.; Pearson, B. D.; Mitra, S.; Bigelow, C. E. *Photochem. Photobiol.* **2005**, *41*, 1544–1547. (e) Geddes, C. D.; Karolin, J.; Birch, D. J. S. *J. Phys. Chem. B* **2002**, *106*, 3835–3841.
(10) (a) Reits, E. A. J.; Neefjes, J. J. *Nat. Cell Biol.* **2001**, *3*, E145–E147. (b) Swaminathan, R.; Bicknese, S.; Periasamy, N.; Verkman, A. S. *Biophys. J.* **1996**, *71*, 1140–1151. (c) Periasamy, N.; Bicknese, S.; Verkman, A. S. *Photochem. Photobiol.* **1996**, *63*, 265–271. (d) Vaz, W. L. C.; Stumpel, J.; Hallmann, D.; Gambacorta, A.; De Rosa, M. *Eur. Biophys. J.* **1987**, *15*, 111–115.

10.1021/cm800702c CCC: $40.75
Published on Web 05/27/2008

Scheme 1. Outline of Procedures Used in the Preparation of the Molecular Rotor

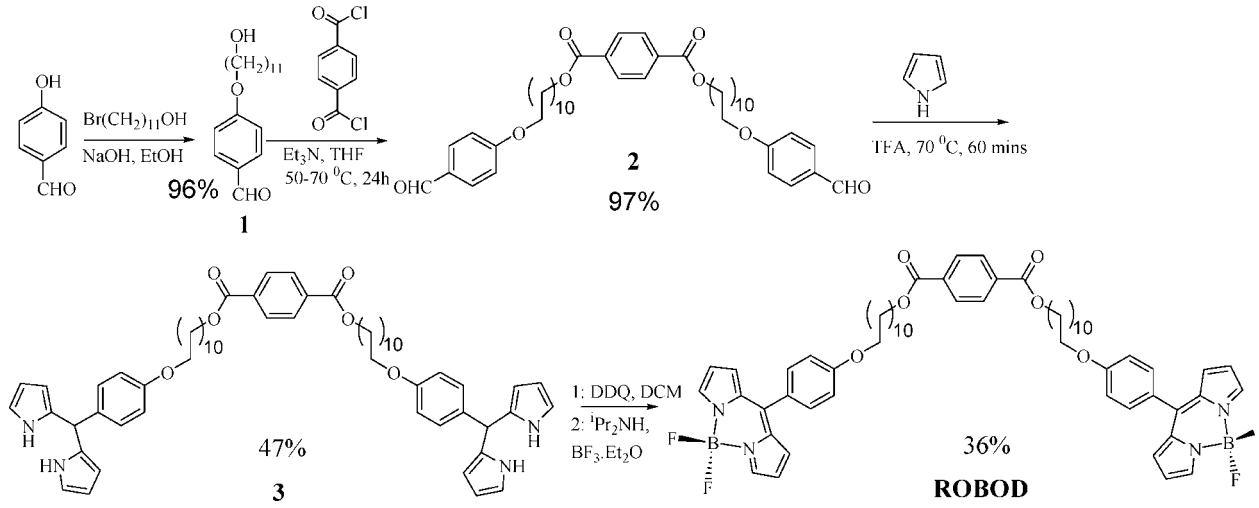

tended toward molecular systems that depend on intramolecular motion. The so-called molecular rotors[11] involving twisted intramolecular charge-transfer (TICT) effects have emerged as extremely valuable fluorescent probes that are sensitive to changes in local viscosity. Several such derivatives have been exploited for commercial purposes. One particular molecule, 9-(dicyanovinyl)-julolidine (DCVJ),[12] is an example in which the TICT state is created following photoinduced charge transfer from the julolidine nitrogen atom to an appended dicyanovinyl group, with concomitant rotation around the julolidine−vinyl bond.[13] It is believed that the TICT state so formed promotes nonradiative deactivation of the fluorescence state. Thus, hindrance of internal motion caused by frictional forces with the local surroundings will suppress TICT formation and restore some of the fluorescence intensity. More recent work,[14] however, has suggested that DCVJ responds to the porosity of the surrounding medium rather than to its actual viscosity. It should also be noted that the absorption and fluorescence profiles characteristic of DCVJ occur in the spectral region from 350 to 500 nm, and are far from ideal for real-time viscosity detection in vivo. Generally, longer-wavelength-absorbing and -emitting species are needed, because the light will be less attenuated by biological tissue.

Seeking to produce improved viscosity-sensitive molecular rotors that avoid TICT (or any other charge-transfer state) formation while possessing absorption and fluorescence transitions localized at more amenable wavelengths, our attention has turned to the boron dipyrromethene (Bodipy) class of dyes.[15] These materials absorb and emit in the 500−700 nm region and, because of the intense, narrow fluorescence profiles and very low triplet yields, have already been proposed as biological probes for many sensor applications.[16] In particular, previous work by Lindsey et al.[17] reported that fluorescence yields for the *meso*-phenyl-substituted Bodipy derivatives were highly dependent on the rotational freedom of the phenyl group. That is to say, restricted rotation of the phenyl by, for example, the introduction of a methyl group proximal to the Bodipy core significantly enhances the fluorescence yield. With this observation in mind, we set out to devise a general-purpose molecular rotor that will respond to changes in the viscosity of the surrounding medium.[18] An obvious advantage of using Bodipy-based dyes is that the basic core can be altered so as to produce a large array of derivatives.[15] To demonstrate the potential of such rotors, we have synthesized a prototype in which two remote Bodipy units are linked by a long flexible chain, **ROBOD** (Scheme 1), and report on its ability to monitor changes in local viscosity. It is not intended that the two head groups interact in any way, and indeed there is no evidence to suggest that they do, but it is anticipated that the elongated structure might facilitate measuring changes in viscous flow,[19] in addition to monitoring shear viscosity.

Experimental Section

Solvents were dried by standard literature methods[20] before being distilled and stored under nitrogen over 4 Å molecular sieves. ^{1}H and ^{13}C NMR spectra were recorded with a Bruker AVANCE 300

(11) Haidekker, M. A.; Theodorakis, E. A. *Org. Biomol. Chem.* **2007**, *5*, 1669–1678.
(12) (a) Lu, J.; Liotta, C. L.; Eckert, C. A. *J. Phys. Chem. A* **2003**, *107*, 3995–4000. (b) Kung, C. E.; Reed, J. K. *Biochemistry* **1986**, *25*, 6114–6121. (c) Lang, M.; Dadali, A. A.; Drickamer, H. G. *Chem. Phys. Lett.* **1993**, *214*, 10–17. (d) Gutkowski, K. I.; Japar, M. L.; Aramendia, P. F. *Chem. Phys. Lett.* **2006**, *426*, 329–333.
(13) (a) Loutfy, R. O.; Arnold, B. A. *J. Phys. Chem.* **1982**, *86*, 4205–4211. (b) Loutfy, R. O.; Law, K. Y. *J. Phys. Chem.* **1980**, *84*, 2803–2808.
(14) Allen, B. D.; Benniston, A. C.; Harriman, A.; Rostron, J. P.; Yu, C. F. *Phys. Chem. Chem. Phys.* **2005**, *7*, 3035–3040.
(15) Bodipy dyes have been developed by Molecular Probes (Invitrogen) for numerous sensing applications (see http://probes.invitrogen.com). For reviews of other uses for bodipy dyes, see: (a) Ziessel, R.; Ulrich, G.; Harriman, A. *New J. Chem.* **2007**, *31*, 496–501. (b) Loudet, A.; Burgess, K. *Chem. Rev.* **2007**, *107*, 4891–4932. (c) Ulrich, G.; Ziessel, R.; Harriman, A. *Angew. Chem., Int. Ed.* **2008**, *47*, 1184–1201.
(16) Rurack, K.; Kollmannsberger, M.; Resch-Genger, U.; Daub, J. *J. Am. Chem. Soc.* **2000**, *122*, 968–969. (b) Yamada, K.; Nomura, Y.; Citterio, D.; Iwasawa, N.; Suzuki, K. *J. Am. Chem. Soc.* **2005**, *127*, 6956–6957. (c) Coskun, A.; Akkaya, E. U. *J. Am. Chem. Soc.* **2005**, *127*, 10464–10465. (d) Malval, J.-P.; Leray, I.; Valeur, B. *New J. Chem.* **2005**, *29*, 1089–1094. (e) Oleynik, P.; Ishihara, Y.; Cosa, G. *J. Am. Chem. Soc.* **2007**, *129*, 1842–1843.
(17) Kee, H. L.; Kirmaier, C.; Yu, L.; Thamyongkit, P.; Youngblood, W. J.; Calder, M. E.; Ramos, L.; Noll, B. C.; Bocian, D. F.; Scheidt, W. R.; Birge, R. R.; Lindsey, J. L.; Holten, D. *J. Phys. Chem. B* **2005**, *109*, 20433–20443.
(18) A small series of bodipy-based dyes have been evaluated for probing viscosity; the increase in fluorescence lifetime, however, by changing the solvent from water to a micelle environment is only ca. 30%. See: (a) Buschmann, V.; Weston, K. D.; Sauer, M. *Bioconjugate Chem.* **2003**, *14*, 195–204.

MHz spectrometer. Chemical shifts for ^{1}H and ^{13}C NMR spectra are referenced with respect to residual protiated solvent. Routine mass spectra were obtained using in-house facilities and elemental analyses were performed at Medac Ltd. Commercial starting materials were purchased from Aldrich Chemical Co. and used as received except for pyrrole, which was redistilled immediately before use.

Absorption spectra were recorded with a Hitachi U3310 spectrophotometer while all fluorescence studies were made with an Yvon-Jobin Fluorolog tau-3 spectrometer. Fluorescence spectra were corrected for spectral imperfections using a standard lamp. Measurements were made using optically dilute solutions after deoxygenation by purging with dried N_2. Fluorescence quantum yields were measured with respect to the corresponding *meso*-pyridyl Bodipy derivative.[21] Corrected excitation spectra were also recorded under optically dilute conditions. Fluorescence lifetimes were measured by time-correlated, single-photon counting conditions following excitation with an ultrashort laser diode emitting at 515 nm. After deconvolution of the instrumental response function, the temporal resolution of this setup was ca. 50 ps. Temperature-dependence studies were made with an Oxford Instruments Optistat DN optical cryostat.

Very high pressure studies were carried out using a custom built rig supplied by Stansted Fluid Power Ltd. and used in conjunction with a high-pressure sample holder equipped with optically transparent windows. Fluorescence measurements were made using a low power laser diode ($\lambda_{max} = 408$ nm) to excite the sample, and collecting emission with a focusing lens connected to a fiber optic cable that was fed to a red-sensitive photomultiplier tube by way of a high-radiance monochromator and amplifier. Scattered excitation light was minimized with optical filters. In a typical run, the sample in an appropriate solvent was pressurized up to ca. 600 MPa. Spectra were measured at regular intervals as the pressure exerted on the sample was released in a controlled manner. Fluorescence background spectra were recorded using solvent only and the final emission spectrum corrected as needed. Several runs were recorded for each solvent. In other runs, the spectra were recorded as the pressure was increased progressively. In all cases, the temperature was maintained at 22 °C.

Preparation of 1. In a 3-necked flask under a nitrogen atmosphere were added 4-hydroxybenzaldehyde (1.83 g, 15.0 mmol), 11-bromoundecan-1-ol (3.96 g, 15.75 mmol) and EtOH (100 mL). The mixture was stirred until the materials had dissolved, and was followed by addition of NaOH (6.43 g, 15.75 mmol) and Bu_4NBr (0.07 g). The mixture was heated at reflux for 2 days, cooled, and the solvent removed. The residue was added to water (100 mL) and subsequently extracted with DCM (3 × 100 mL). The organic layer was separated, dried over $MgSO_4$, filtered, and removed to afford a residue that was purified by column chromatography using petroleum ether/EtOAc (4:1) as eluent to give a white solid. Yield 4.2 g, 96%. Mp = 63−65 °C. ^{1}H NMR ($CDCl_3$, 300 MHz): δ 9.87 (1H, s), 7.84 (2H, d, J = 8.7 Hz), 6.99 (2H, d, J = 8.7 Hz), 4.03 (2H, t, J = 6.5 Hz), 3.64 (2H, t, J = 6.6 Hz), 1.81(2H, m), 1.59−1.29 (12H, m). ^{13}C NMR ($CDCl_3$, 75 MHz): δ 190.29, 164.06, 131.59, 129.63, 115.76, 114.58, 68.21, 62.25, 62.37, 32.45, 29.21, 29.13, 28.95, 28.75, 25.61, 25.49. IR (cm^{-1}) 2918, 2851 (C−H), 1677, 1602, 1576.

Preparation of 2. To a 3-necked flask under a nitrogen atmosphere containing THF (200 mL) were added derivative **1** (4.39 g, 15 mmol) and terephthaloyl chloride (1.52 g, 7.5 mmol). Triethylamine (35 mL) was added and the reaction stirred for 2 h at room temperature, then for another 24 h at 50−70 °C. The solvent was removed and water (100 mL) added, before the mixture was extracted with DCM (3 × 120 mL). The organic layer was separated, dried over $MgSO_4$, filtered, and evaporated to afford the crude product. Purification of this material by column chromatography on silica gel using EtOAc/petroleum ether/DCM (1:3:0 to 1:3:1) as eluent afforded a white solid. Yield 5.20 g, 97.0%. Mp = 91−93 °C. ^{1}H NMR ($CDCl_3$, 300 MHz): δ 9.87 (2H, s), 8.09 (4H, s), 7.84 (4H, d, J = 8.7 Hz), 6.99 (4H, d, J = 8.7 Hz), 4.33 (4H, t, J = 6.5 Hz), 4.03 (4H, t, J = 6.5 Hz), 1.83−1.75 (8H, m, CH_2), 1.46−1.32 (28H, m, CH_2). ^{13}C NMR ($CDCl_3$, 75 MHz): δ 190.43, 165.88, 164.38, 134.47, 131.89, 130.18, 129.49, 114.94, 68.58, 65.55, 29.48, 29.32, 29.25, 29.15, 28.78, 26.04, 26.01. IR (cm^{-1}) 2921, 2853 (C−H), 1711 (C═O).

Preparation of 3. To a 3-necked flask under a nitrogen atmosphere were added **2** (3.57 g, 5.0 mmol), pyrrole (17.7 mL, 250 mmol), and TFA (0.077 mL, 1.0 mmol). The mixture was stirred at room temperature for 10 min, followed by raising the temperature to 70 °C for 60 min. The mixture was cooled to room temperature and excess pyrrole was removed by distillation under reduced pressure. The residue was passed through a short column of aluminum oxide, using DCM/EtOAc (1:0 to 3:1) as eluent, to afford a brown solid. Yield 2.2 g, 47%. ^{1}H NMR ($CDCl_3$, 300 MHz): δ 8.10 (4H, s), 7.94 (4H, br, NH), 7.12 (4H, d, J = 7.6 Hz), 6.84 (4H, d, J = 7.6 Hz), 6.69 (4H, dd, J = 2.6 Hz, J = 4.1 Hz), 6.16 (4H, dd, J = 2.7 Hz, J = 5.8 Hz), 5.91 (4H, m), 5.42 (2H, s), 4.33 (4H, t, J = 6.5 Hz), 3.92 (4H, t, J = 6.5 Hz), 1.78−1.76 (8H, m), 1.44−1.31(28H, m). ^{13}C NMR ($CDCl_3$, 75 MHz): δ 165.89, 158.39, 134.47, 134.27, 133.00, 129.49, 129.39, 117.00, 114.89, 108.59, 107.15, 68.32, 65.57, 43.450, 29.52, 29.48, 29.41, 29.38, 29.26, 28.00, 26.12, 26.06.

Preparation of ROBOD. To a stirred solution of **3** (1.2 g, 1.26 mmol, 1 eq.) in DCM (500 mL) at room temperature was added DDQ (1.71 g, 7.6 mmol, 6 equiv.). An immediate color change from light brown to a very dark brown was observed. When TLC (silica: DCM) showed complete consumption of the starting material, *N*,*N*-diisopropylethylamine (2.4 mL, 14 mmol, 11.4 equiv.) and $BF_3 \cdot Et_2O$ (2.55 mL, 20 mmol, 16 equiv.) were added, and the reaction was stirred for 6 h at room temperature. The reaction mixture was washed with water (3 × 100 mL) and brine (3 × 100 mL). The separated organic fractions were dried ($MgSO_4$), filtered, and evaporated to give the crude product. This material was chromatographed on silica gel using DCM as eluent. Collection of the desired fraction followed by solvent removal afforded a solid that was washed with petroleum ether, filtered and dried to give a dark red compound (0.46 g, 36% yield). Mp = 48−51 °C. ^{1}H NMR ($CDCl_3$, 300 MHz): δ 8.02 (s, 4H), 7.83 (broad s, 4H), 7.44 (d, J = 8.7 Hz, 4H), 6.94 (d, J = 8.7 Hz, 4H), 6.88 (d, J = 4 Hz, 4H), 6.46 (dd, J = 7.8 Hz, J = 1.5 Hz, 4H), 4.26 (t, J = 6.7 Hz, 4H), 3.96 (t, J = 6.7 Hz, 4H), 1.73 (m, 8H), 1.32 (m, 28H). ^{13}C NMR ($CDCl_3$, 75 MHz): δ 166.14, 162.22, 147.96, 143.70, 135.36, 134.78, 132.73, 131.58, 129.78, 126.64, 118.42, 115.03, 68.86, 65.83, 29.80, 29.77, 29.65, 29.54, 29.08, 26.37, 26.34. MALDI-MS m/z = 1038. Elemental analysis calcd (%) for $C_{60}H_{68}B_2F_4N_4O_6$: C, 69.37; H, 6.60; N, 5.39. Found: C, 69.38; H, 6.54; N, 5.52.

Results and Discussion

Synthesis and Structure. The procedures used to prepare the title compound are outlined in Scheme 1, starting from commercially available 4-hydroxybenzaldehye. This com-

(19) (a) Quintella, C. M.; Musse, A. P. S.; Gonçalves, C. C.; McCaffery, A. *J. Expt. Fluids* **2003**, *35*, 41–48. (b) Valeur, B. *Molecular Fluorescence*; Wiley-VCH: Weinheim, Germany, 2001; Chapter 8.
(20) Riddick, J. A.; Bunger, W. B.; Sakano, T. K. *Organic Solvents*, 4th ed.; Wiley-Interscience, New York, 1986.
(21) Harriman, A.; Mallon, L. J.; Ulrich, G.; Ziessel, R. *ChemPhysChem* **2007**, *8*, 1207–1214.

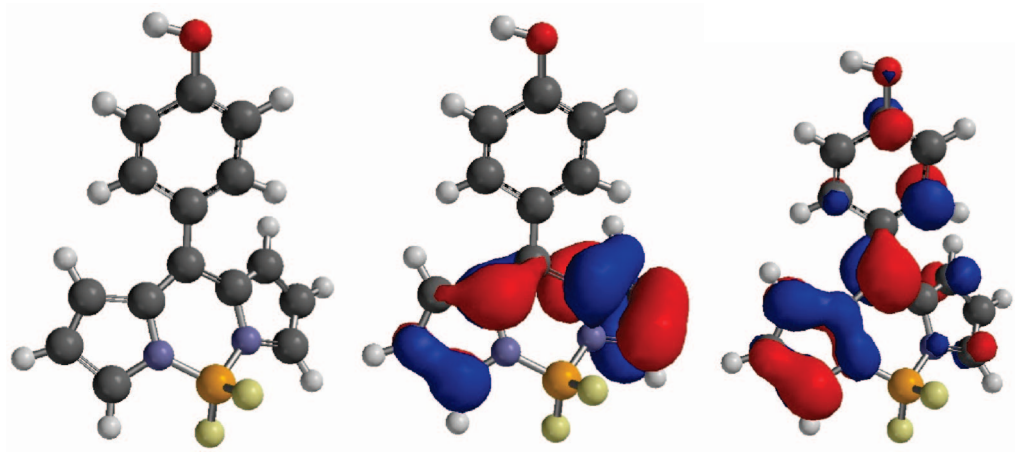

Figure 1. (Left) Computed geometry for the most distorted dipyrrin structure observed in the MDS runs for full rotation of the meso-phenyl ring. Computed electron density map for the HOMO (center) and LUMO (right) for the distorted geometry.

pound was converted to the alcohol **1** in excellent yield by deprotonation and reaction with 11-bromoundecan-1-ol. It is conceivable at this stage to introduce the Bodipy unit, but instead we opted to construct the dialdehyde derivative **2**, by coupling **1** with terephthaloyl chloride in the presence of base. The yield for this reaction was also excellent. Reaction of **2** with excess pyrrole in the presence of acid afforded the dipyrrylmethane derivative **3**, which was readily converted to the desired compound **ROBOD** using standard procedures. Although the yields of the final two steps are low (17% overall), derivative **3** could be made on the several gram-scale, and hence scale-up to produce workable quantities of **ROBOD** is entirely feasible. The final compound is soluble in most common organic solvents, but clearly not in water, and stable upon prolonged storage. Purification is readily accomplished by column chromatography on silica gel using CH_2Cl_2 as eluent. Repeated TLC on silica gel using CH_2Cl_2 as the mobile phase can be used as a means to obtain small samples of highly purified material for photophysical studies. The most notable features of the ^{1}H NMR spectra are the two clear triplets at 4.3 and 3.9 ppm; these can be assigned to the two different methylene groups adjacent to the oxygen atoms. The MALDI mass spectrum of the title compound is dominated by a strong molecular ion at $m/z = 1038.5$, with clear fragmented ion peaks at 1019.5 and 1000.6 corresponding to sequential loss of fluorine atoms. The absorption spectrum shows clear transitions to the first ($\lambda = 496$ nm) and second ($\lambda = 405$ nm) excited-singlet states but there are no indications for association between the two Bodipy head groups, despite the fact that Bodipy dyes are known to self-associate under certain conditions.[22]

As a key feature by which to form a molecular rotor, the alkyl groups usually found on the pyrrole units have to be omitted.[17] The energy-minimized geometry, computed at the AM1 level, has the *meso*-phenyl ring held at an average angle of 49° to the plane of the Bodipy unit. The latter core is planar and free of obvious stereochemical strain. The computed structure shows the expected tetrahedral arrangement around the boron center, with B−F bond lengths (i.e., 1.342 Å) and angles (i.e., 108.8°) consistent with single-crystal X-ray data collected for other Bodipy dyes.[23] The ability of the *meso*-phenyl ring to rotate around the connecting C−C bond was confirmed by molecular dynamics simulations (MDS) made *in vacuo* and in a solvent reservoir. The rotational barrier for the solute dispersed in a solvent bath was calculated to be 45 kJ/mol. Close examination of structures computed for planar and orthogonal geometries shows that complete rotation of the phenyl ring is accompanied by a slight curvature of the Bodipy framework (Figure 1). Thus, the upper rim of the dipyrrin nucleus undergoes a minor deflection away from planarity that allows the *meso*-phenyl ring to adopt a geometry that is essentially planar with the lower rim of the dipyrrin. At this point, the connecting dihedral angle is essentially zero and quantum chemical calculations indicate that the LUMO now has considerable electron density on the phenyl ring (Figure 1).

Photophysical Properties. The absorption spectrum, and molar absorption coefficient ($\epsilon_{MAX} = 141{,}000$ M^{-1} cm^{-1}), recorded for **ROBOD** in ethanol solution are as expected[24] for a Bodipy dye (Figure 2). The absorption maximum ($\lambda_{MAX} = 496$ nm) lies at slightly higher energy than usually associated with such dyes, because of the lack of an inductive effect from the alkyl groups on the dipyrrin unit. It is notable that the optical transition from the ground state to the second excited singlet state, which is centered at 405 nm, is more pronounced than normally found for Bodipy dyes.[25] This feature is probably a consequence of the reduced splitting between the two states. The fluorescence spectrum shows good mirror symmetry with the lowest-energy absorption band and there is excellent agreement between absorption and excitation spectra across the entire spectral range. The fluorescence maximum (λ_{FLU}) lies at 514 nm, such that Stokes' shift is kept to a minimum (SS = 705 cm^{-1}). Interestingly, the fluorescence quantum yield ($\Phi_F = 0.049$) determined in ethanol solution at room temperature is considerably reduced with respect to Bodipy dyes bearing

(22) (a) Dahim, M.; Mizuno, N. K.; Li, X.-M.; Momsem, W. E.; Momsem, M. M.; Brockman, H. L. *Biophys. J.* **2002**, *83*, 1511–1524. (b) Ji, D.; Zhao, R.; Huang, Z.; Xia, A. *J. Lumin.* **2006**, *122*, 253–255. (c) Harriman, A.; Mallon, L. J.; Stewart, B.; Ulrich, G.; Ziessel, R. *Eur. J. Org. Chem.* **2007**, 3191–3198.

(23) Harriman, A.; Rostron, J. P.; Cesario, M.; Ulrich, G.; Ziessel, R. *J. Phys. Chem. A* **2006**, *110*, 7994–8002.

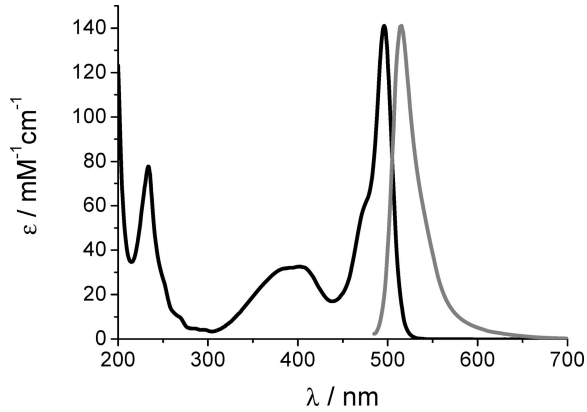

Figure 2. Overlay of absorption (black) and fluorescence (gray) spectra recorded for **ROBOD** in ethanol solution at room temperature.

alkyl substituents at the pyrrole rings.[24] There is a corresponding reduction in the fluorescence lifetime ($\tau_F = 0.36$ ns) but the radiative rate constant ($k_{RAD} = \Phi_F/\tau_F$) is comparable to values found for other Bodipy dyes.[24] Furthermore, the radiative rate constant ($k_{RAD} = 1.3 \times 10^8$ s^{-1}) calculated from the Strickler−Berg expression[26] is in excellent agreement with that found experimentally ($k_{RAD} = 1.4 \times 10^8$ s^{-1}). It appears, therefore, that there is an additional nonradiative deactivation channel open to **ROBOD** that is closed to Bodipy dyes bearing alkyl groups at the pyrrole rings. This finding is consistent with the idea of **ROBOD** acting as a molecular rotor, as has been suggested[17] previously for simpler derivatives of related Bodipy dyes. Indeed, the Φ_F and τ_F found for **ROBOD** are in general agreement with data reported by Lindsey et al.[17] for sterically unhindered Bodipy derivatives, where Φ_F tends to be around 0.06 and τ_F is in the region of 0.6 ns in toluene solution at room temperature.

To examine this additional nonradiative process in more detail, the photophysical properties of **ROBOD** were measured in a series of linear alcohols at 20 °C and the main findings are collected in Table 1. Throughout this series of solvents, k_{RAD} remains reasonably constant, as does the magnitude of the Stokes' shift, but both Φ_F and τ_F vary progressively with the bulk viscosity of the solvent (η). The variation in Φ_F agrees well with the Förster−Hoffmann expression[27] (eq 1), where the coefficient β has a value of 0.44 and C (= −1.30) is a constant (see the Supporting Information, Figure S1). This former term is used to indicate that bulk viscosity is an inappropriate measure of solute−solvent interactions and should be replaced with microviscosity.[28] The actual magnitude of β indicates the sensitivity of the probe to changes in viscosity. Indeed, the variation in Φ_F with increasing viscosity is about 50% more pronounced than that found for DCVJ under the same experimental conditions, showing **ROBOD** to be a superior probe of solvent viscosity. However, it should be stressed that the Förster−Hoffmann expression[27] is a rather crude measure of the probe's performance and, although widely used, is not strictly valid since it predicts nonexponential decay kinetics. For **ROBOD** in linear alcohols, the decay profiles remain strictly exponential. Under these conditions, eq 2 provides a better measure of how the rotor responds to changes in local viscosity.[29] Here, υ is the limiting pressure exerted by the rotor, α is a coefficient that describes frictional forces between rotor and surrounding solvent, and E_A is the activation energy for internal rotation. The rate constant for nonradiative decay of the excited-singlet state (k_{NR}) is obtained according to eq 3. From the linear fit to eq 2 (see the Supporting Information, Figure S2), α has a value of 0.44, which can be compared with $\alpha = 0.30$ for DCVJ under identical conditions and thereby confirms the impression that **ROBOD** is a superior probe by which to monitor changes in solvent viscosity. There is, however, a substantial increase in both Φ_F and τ_F in toluene relative to methanol (Table 1), although their viscosities are the similar, which could be taken to indicate that factors other than the bulk viscosity are important in setting the fluorescence properties of the solute.

Table 1. Effect of Solvent Viscosity on the Photophysical Properties of ROBOD in Normal Alcohols and Toluene at 20 °C

solvent	λ_{MAX} (nm)	λ_{FLU} (nm)	η (cP)	Φ_F	τ_F (ns)	k_{RAD} (× 10^8 s^{-1})	k_{NR} (× 10^9 s^{-1})
CH_3OH	495	512	0.54	0.038	0.32	1.2	3.0
C_2H_5OH	496	514	0.69	0.049	0.36	1.4	2.7
C_3H_7OH	497	514	1.95	0.057	0.43	1.3	2.2
C_4H_9OH	497	514	2.54	0.071	0.59	1.2	1.6
$C_5H_{11}OH$	498	515	3.62	0.082	0.63	1.3	1.5
$C_6H_{13}OH$	499	515	4.58	0.096	0.63	1.5	1.4
$C_7H_{15}OH$	499	515	5.81	0.108	0.70	1.5	1.3
$C_8H_{17}OH$	499	515	7.29	0.134	0.84	1.6	1.0
$C_{10}H_{21}OH$	499	517	10.90	0.142	0.93	1.5	0.92
Toluene	501	522	0.59	0.084	0.75	1.1	1.2

$$\log \Phi_F = C + \beta \log \eta \tag{1}$$

$$k_{NR} = \frac{\upsilon}{\eta^{\alpha}} \exp\left(-\frac{E_A}{RT}\right) \tag{2}$$

$$k_{NR} = \frac{1 - \Phi_F}{\tau_F} \tag{3}$$

The fluorescence quantum yield measured for **ROBOD** in ethanol increases with decreasing temperature, reaching a value close to unity in the glassy matrix (Figure 3). This latter finding confirms the generic belief that intersystem crossing to the triplet manifold is ineffective for this class of dye and indicates that τ_F approaches the inverse of k_{RAD} in the glass. It also points to the importance of the viscosity-controlled nonradiative decay route in setting the photophysical properties at ambient temperature. The spectral profile does not change with temperature, but there is a 2 nm blue shift upon cooling from 323 to 120 K. The

(24) (a) Vos de Wael, E.; Pardoen, J. A.; van Koeveringe, J. A.; Lugtenburg, J. *Recl. Trav. Chim. Pays-Bas* **1977**, *96*, 306–309. (b) Kollmannsberger, M.; Rurack, K.; Resch-Genger, U.; Daub, J. *J. Phys. Chem. A* **1998**, *102*, 10211–10220. (c) Costela, A.; Garcia-Moreno, I.; Gomez, C.; Sastre, R.; Amat-Guerri, F.; Liras, M.; Lopez Arbeloa, F.; Banuelos Prieto, J.; Lopez Arbeloa, I. *J. Phys. Chem. A* **2002**, *106*, 7736–7742. (d) Qin, W.; Baruah, M.; Van der Auweraer, M.; De schryver, F. C.; Boens, N. *J. Phys. Chem. A* **2005**, *109*, 7371–7384.
(25) Ziessel, R.; Goze, C.; Ulrich, G.; Cesario, M.; Retailleau, P.; Harriman, A.; Rostron, J. P. *Chem.—Eur. J.* **2005**, *11*, 7366–7378.
(26) Strickler, S. J.; Berg, R. A. *J. Chem. Phys.* **1962**, *37*, 814–820.
(27) Haidekker, M. A.; Akers, W.; Lichlyter, D.; Brady, T. P.; Theodorakis, E. A. *Sens. Lett.* **2005**, *3*, 42–48.
(28) Dale, R. E.; Chen, L. A.; Brand, L. *J. Biol. Chem.* **1977**, *252*, 7500–7510.
(29) Baggi, B. *Int. Rev. Phys. Chem.* **1987**, *6*, 1–34.

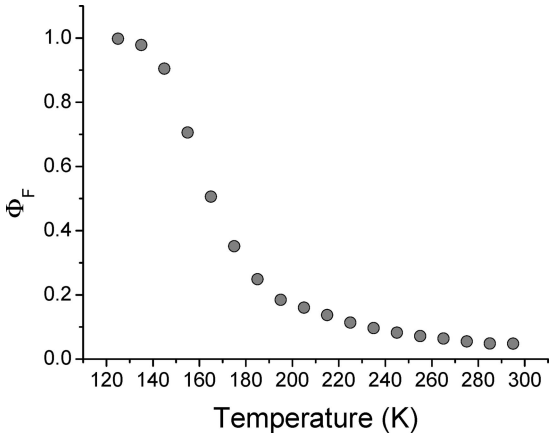

Figure 3. Effect of temperature on the fluorescence quantum yield measured for **ROBOD** in ethanol solution.

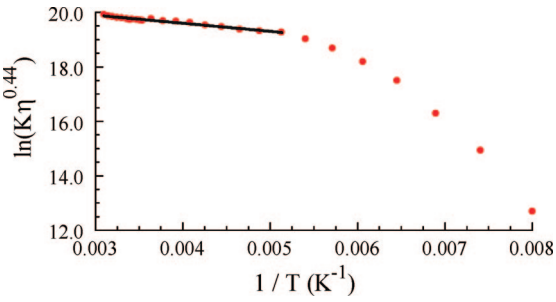

Figure 4. Arrhenius-type plot showing the effect of temperature on the "viscosity-corrected" rate constant for nonradiative decay of **ROBOD** in ethanol solution.

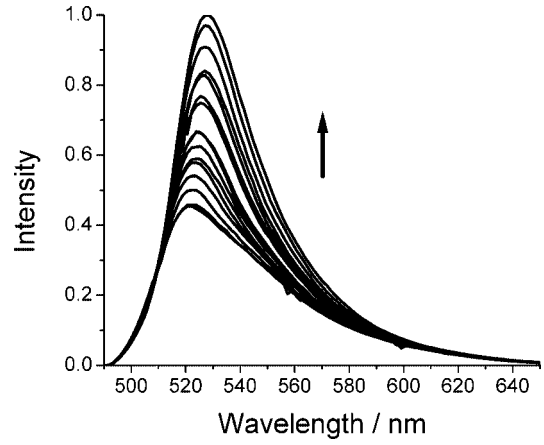

Figure 5. Effect of applied pressure on the fluorescence spectral profile of **ROBOD** in methanol solution. The pressure varies progressively from 1 to 550 MPa, causing an increase in fluorescence intensity and a slight red shift.

temperature effect is presumably related to the increase in viscosity that accompanies cooling of the solvent and, in principle, it should be possible to correct eq 2 for temperature-induced changes in viscosity and thereby obtain an estimate for the barrier height (E_A). The viscosity of ethanol does not follow simple Arrhenius behavior over such a wide temperature range,[30] however, and is best described in terms of eq 4, where A (= −5.9052), B (= 1922.5), and C (= 189.7) are free parameters obtained from least-squares fitting of experimental data.[31] Using such interpolated viscosities, and assuming that α is independent of both temperature and viscosity, the form of eq 2 was compensated for temperature-imposed changes in viscosity in order to expose the barrier to rotation (E_A). The resultant fit to eq 2 is nonlinear (Figure 4).

At low temperature, where the viscosity is high, nonradiative decay is strongly activated, but this is not the case at ambient temperature. Indeed, at the high temperature limit (Figure 4), the barrier for gyration of the phenyl ring in the excited singlet state is only 2.5 kJ mol^{-1}; this is much lower than the value found by Lindsey et al.[17] with a sterically unhindered Bodipy dye dispersed in a plastic medium, where E_A = 12 kJ mol^{-1}. Overall, these findings are consistent with a high rotation barrier at very high viscosity but a rather small barrier in fluid solution. Further insight into this unusual behavior was sought from isothermal pressure-dependent studies.

$$\log \eta = A + \frac{B}{(T + C)} \tag{4}$$

High-Pressure Studies. To further examine how the environment affects the photophysical properties of **ROBOD** in fluid solution, we made a series of high-pressure studies. Here, the fluorescence yield was recorded as a function of applied pressure, and a typical set of results is given as Figure 5. It can be seen that the applied pressure has little effect on the spectral profile, at least in linear alcohols, but causes a slight red shift in some solvents and an increase in the fluorescence intensity in all cases. In methanol, for example, there is a 75% increase in the fluorescence intensity on raising the pressure from atmospheric to 550 MPa and a concomitant red shift in the emission maximum of ca. 6 nm. The solvent does not freeze under these conditions but undergoes a marked increase in viscosity[32] and a modest change in refractive index.[33] There is a corresponding 4 nm red shift in the absorption maxima for both S_0-S_1 and S_0-S_2 transitions over the same pressure range (see the Supporting Information). The pressure-induced changes in absorption and fluorescence spectra are fully reversible, provided the solute is adequately soluble in that particular solvent, and highly reproducible. Similar effects are observed in a range of linear alcohols, with the actual increase in fluorescence yield being dependent on the nature of the solvent. In methanol, the fluorescence changes are a linear function of the applied pressure, at least to a first approximation, but this linear relationship is seen only for the shorter alcohols. For the longer alcohols, there is positive deviation from linearity and only a slight effect on the position of the emission maximum as the pressure is increased (see the Supporting Information).

We have shown above that the fluorescence yield (and lifetime) increases with increasing viscosity, and it is well-established that most solvents undergo an increase in

(30) Petravic, J.; Delhommelle, J. *J. Chem. Phys.* **2005**, *122*, 234509.
(31) Gutmann, F.; Simmons, L. M. *J. Appl. Phys.* **1952**, *23*, 977–978.
(32) Schmelzer, J. W. P.; Zanotto, E. D.; Fokin, V. M. *J. Chem. Phys.* **2005**, *122*, 74511.
(33) Paul, G. R.; Cameron, A. *Proc. R. Soc. London, Ser. A* **1972**, *331*, 171–184.

Table 2. Effect of Applied Pressure on the Fluorescence Spectral Properties of ROBOD **Recorded in Methanol Solution**

pressure (MPa)	λ_{FLU} (nm)	SS (cm^{-1})	ν_{0-1} (cm^{-1})[a]	S
0	519	1128	19455	0.45
83	521	971	19406	0.46
165	521	951	19382	0.47
248	522	852	19354	0.48
303	522	910	19317	0.49
359	522	875	19308	0.49
414	523	870	19311	0.48
496	523	850	19250	0.51
552	524	830	19260	0.50

[a] Wavenumber corresponding to the highest-energy Gaussian component found by spectral deconvolution.

viscosity as the applied pressure is raised progressively.[34] In some cases, it has been shown[35] that there is a linear relationship between viscosity and applied pressure, although the underlying theoretical reasoning for this effect is poorly understood.[36] The observed pressure effect on fluorescence intensity, therefore, is easily assigned to changes in viscosity. It is also known from earlier work[37] with related Bodipy dyes that the emission maximum is affected by changes in the polarizability of the solvent (see the Supporting Information). Indeed, a linear relationship is generally observed between the emission peak and the Lorentz−Lorenz polarizability function (f_L);[38] defined by eq 5 with n being the refractive index of the solvent. Usually, the wavenumber corresponding to the peak maximum (ν_{FLU}) of a particular Bodipy-based dye decreases with increasing f_L but the magnitude of the shift is rather small.[37] Even so, we can use the pressure-induced spectral changes observed for **ROBOD** to calibrate the system as a means by which to monitor changes in both viscosity and refractive index. For example, in the specific case of methanol, the increase in fluorescence yield found at 550 MPa corresponds to a 3-fold increase in viscosity such that the effective Φ_F is comparable to that found in *n*-propanol at atmospheric pressure. Likewise, a 6 nm red shift corresponds to a change in refractive index of the medium from 1.329 at atmospheric pressure to 1.400 at 550 MPa, and a corresponding decrease in f_L.

$$f_L = \frac{n^2 - 1}{n^2 + 2} \tag{5}$$

Closer examination of the emission spectra recorded in ethanol indicates that an increased pressure causes subtle changes additional to those highlighted above (Table 2). Most notable are an increase in the Huang−Rhys factor[39] (S) and a decrease in the magnitude of the low-frequency vibrational mode ($h\omega_L$) coupled to decay of the S_1 state. Both of these parameters can be derived from spectral curve-fitting routines[40] carried out as a function of applied pressure (see the Supporting Information). There is also a small, but definite, increase in the total reorganization energy (λ_T) associated with formation of the relaxed S_1 state following illumination, as measured from changes in the Stokes' shift.[41] These effects are interrelated: Thus, the overall reorganization energy ($\lambda_T = \lambda_N + \lambda_S$) includes contributions from nuclear (λ_N) and solvent (λ_S) terms. The slightly increased reorganization energy is most likely a consequence of the difference in polarizability of the ground and excited states and is therefore related to a small increase in λ_S. The Huang−Rhys factor ($S = \lambda_N/h\omega_L$) is related to both the nuclear term and the coupled vibronic frequency such that its increase with increasing pressure is easily explained. It is this latter term that shows the most sensitivity toward changes in pressure, and it is clear that increasing pressure causes the corresponding vibrational force constant to decrease. Presumably, the coupled vibronic mode relates to the gyroscopic motion of the *meso*-phenyl ring and an increased pressure will raise the resistance toward such an action. The pressure-induced changes in the spectral profile, therefore, can be traced to a slight increase in refractive index, which itself is due to an increase in the density of the solvent,[42] and to an increased resistance to rotation of the *meso*-phenyl ring, which is also related to an increased density.

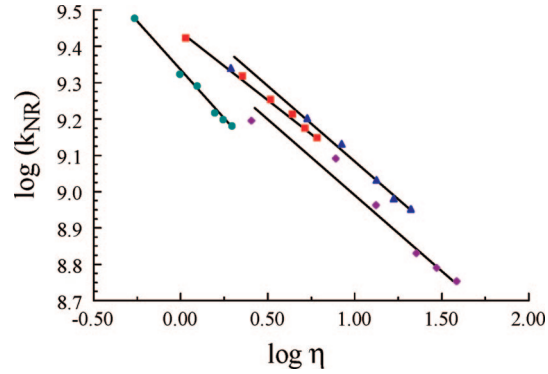

Figure 6. Effect of pressure-induced changes in viscosity on the rate constant for nonradiative decay of **ROBOD** in some normal alcohols. Solvents are methanol (●), ethanol (■), propanol (▲), and butanol (♦) at applied pressures of 1, 140, 275, 410, 480, and 550 MPa.

We return now to the observation that there is an increase in fluorescence yield with increasing applied pressure in all solvents. To examine this feature in more detail, we compared the fluorescence results with the literature viscosity value[43] determined by a more conventional technique, such as the rolling sphere method. This comparison was made for the series of alcohols from methanol to pentanol, where the pressure effect on shear viscosity is well-known. At any given pressure, the fit to eq 2 is nonlinear and k_{NR} tends toward a limiting value at low viscosity. Restricting attention to a particular solvent gives a linear fit to eq 2 for the shorter alcohols, methanol and ethanol, but the fit becomes increasing more nonlinear for the longer analogues (Figure 6). This is clear indication that the observed viscosity effect is solvent sensitive. Furthermore, there is considerable variation in the value of k_{NR} at $\eta = 1$ Pa s. This inferred rate constant, which contains information on both the limiting pressure v and the

(34) Grocholski, B.; Jeanloz, R. *J. Chem. Phys.* **2005**, *123*, 204503.
(35) Bridgman, P. W. *Proc. Am. Acad. Arts Sci.* **1926**, *61*, 57–70.
(36) Kapoor, K.; Dass, N. *J. Appl. Phys.* **2005**, *98*, 66105.
(37) Qin, W.; Rohand, T.; Baruah, M.; Stefan, A.; Van der, Auweraer.; Dehaen, W.; Böens, N. *Chem. Phys. Lett.* **2006**, *420*, 562–568.
(38) Narger, U.; de Bruyn, J. R.; Stein, M.; Balzarini, D. A. *Phys. Rev. B* **1989**, *39*, 11914–11919.
(39) Guha, S.; Rice, J. D.; Yau, Y. T.; Martin, C. M.; Chabdrasekhar, M.; Chandrasekhar, H. R.; Guentner, R.; Scanduicci de Freitas, P.; Scherf, U. *Phys. Rev. B* **2003**, *67*, 125204–125211.
(40) Harriman, A.; Izzet, G.; Goeb, S.; De Nicola, A.; Ziessel, R. *Inorg. Chem.* **2006**, *45*, 9729–9741.
(41) Englman, R.; Jortner, J. *Mol. Phys.* **1970**, *18*, 145–164.
(42) Matyushov, D. V. *J. Chem. Phys.* **2004**, *120*, 7532–7556.
(43) Grocholski, B.; Jeanloz, R. *J. Chem. Phys.* **2005**, *123*, 204503.

barrier to gyration E_A, does not vary smoothly with the size of the alcohol but shows and is a reasonable correlation between the intercept and the module of all-round compression of the solvent.[44] This latter term, which is the inverse of the isothermal compressibility, is a measure of the elasticity of the medium and increases steadily with increasing molar mass for the linear alcohols.

Polymerization, Viscous Flow, and Polarization. Polymerization of a monomer at ambient temperature leads to a significant increase in viscosity of the medium. It was found that the fluorescence intensity recorded for **ROBOD** in methyl methacrylate was insensitive to storage time unless a free-radical initiator was added. In this case, the fluorescence intensity increased progressively as the monomer began to polymerize. The rate of the fluorescence increase depends on temperature and reflects the rate of polymerization (see the Supporting Information). This is a particularly simple way to monitor the rate of polymerization in real-time. A similar response was used to measure the onset of gelation, melting, freezing and a phase change. In each case, **ROBOD** undergoes a reversible modulation in fluorescence intensity as the viscosity varies. The ability of **ROBOD** to measure fluid velocity was examined using a syringe pump, but it was observed that the fluorescence intensity did not change systematically with flow rate. Studies were made in ethanol, pentanol, and octanol but with the same negative result. In other work[19] where the fluorescence sensor does respond to viscous flow, the sensor has been equipped with an ionizable group at the periphery, often this being a carboxylate group, and this feature might be essential for recording viscous drag.

$$P = \frac{F_V - F_H}{F_V + F_H} \tag{6}$$

The degree of fluorescence polarization (P) recorded for an organic fluorophore in fluid solution can be expressed[45] in terms of eq 6 where F_V and F_H, respectively, refer to the vertical and horizontal components of the emission signal. This term can be related to bulk viscosity on the basis that the degree of polarization depends on the rotational relaxation time of the emitter. For the Bodipy-based reference compound having a sterically blocked *meso*-phenyl ring in methanol solution, there is a small increase in P with increasing applied pressure (Figure 7). Extrapolation to infinitely high pressure infers that the limiting value of P will be around 0.4 but this is restricted to a 2-fold increase in P over the pressure range available to us. Now, for **ROBOD**, the initial polarization value is much higher than for the reference compound because the fluorescence lifetime is much shorter. Unlike the reference, this lifetime increases with increasing pressure and tends to offset the effect of increasing viscosity on the rotational relaxation time. It is notable that gyration of the *meso*-phenylene ring plays no part in fluorescence polarization because this unit lies orthogonal to the direction of the transition moment. The net result is that P becomes essentially independent of the applied pressure. This disparate behavior found for **ROBOD**

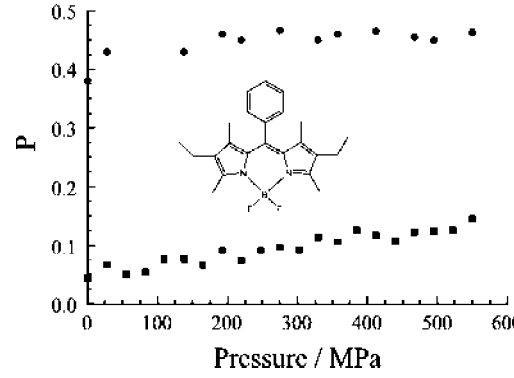

Figure 7. Effect of applied pressure on the degree of fluorescence polarization recorded for (●) **ROBOD** and (■) the reference compound. The molecular formula of the latter is shown on the figure.

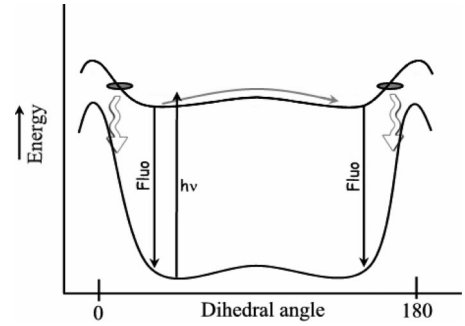

Figure 8. Potential energy diagram proposed to explain the behavior of **ROBOD** in a fluid solvent. The key feature is a flattened surface for the S_1 state that contains drain holes for coupling to the S_0 surface.

and the reference compound is insufficient to be exploited as a means to enhance the sensitivity of the probe to changes in local viscosity.

Mechanism. Overall, this work has confirmed an earlier finding[17] that sterically unhindered, meso-substituted Bodipy dyes are weakly fluorescent because of the availability of an effective nonradiative decay channel that involves gyration of the aryl substituent and accompanying distortion of the dipyrrin superstructure. These internal motions are subject to frictional forces with the surrounding medium such that the emission properties are related to changes in temperature, pressure, and viscosity. Interestingly, it is clear that the actual fluorescence lifetimes and yields are dependent on the nature of the medium, not just on the external conditions. The main argument presented in this work is that the fluorescence yield and lifetime can be used to report on the condition of the surrounding medium but, in order to develop improved reporters, it is necessary to understand why ring gyration presents an important deactivation route for the fluorescent state. It is clear that nonradiative decay is related to conformational changes and, because Bodipy dyes bearing methyl groups on either aryl ring or dipyrrin unit do not show the same effects, we raise the obvious conclusion that the main structural change relates to distortion of the dipyrrin framework. A potential energy diagram calculated for rotation of the *meso*-phenyl ring in the ground-state dye is shown as Figure 8. The barrier to complete rotation is calculated to be 45 kJ/mol and there is also a small barrier to attaining the fully orthogonal geometry. This latter barrier,

(44) Schmelzer, J. W. P.; Zanotto, E. D.; Fokin, V. M. *J. Chem. Phys.* **2005**, *122*, 74511.
(45) Mann, T. L.; Krull, U. J. *The Analyst* **2003**, *128*, 313–317.

calculated to be ca. 3 kJ/mol, arises because of the desire to spread the LUMO over the *meso*-aryl ring, which is prevented by the perpendicular geometry (see the Supporting Information). The preferred dihedral angle for the *meso*-phenyl ring in the ground-state is 49° and MDS studies indicate that the phenyl ring flips between the two stable states either side of the orthogonal arrangement (see the Supporting Information). The form of Figure 8 is reminiscent of that reported by Lindsey et al.[17] and appears to give a good description of the ground-state of these unhindered Bodipy dyes. The main point, however, is establishing how this potential energy surface differs from that for the excited-singlet state.

Several potential energy profiles for S_1 need to be considered in order to rationalize all the available experimental data. Lindsey et al.[17] computed a convex profile with an energy-minimized geometry having the *meso*-phenyl ring held at 180° so as to maximize electron delocalization over the entire structure. The shape of this profile does not easily account for the relatively slow rates of nonradiative decay found for **ROBOD** or the temperature dependence. Various shapes for barrierless S_1 potential surfaces have been reviewed in detail by Ben-Amotz and Harris[46] for triphenyl methane dyes and include three generic types; namely, the flat potential model introduced by Oster−Nishijima,[47] and the parabolic potentials coupled to local or nonlocal pinhole sinks suggested by Forster−Hoffman[48] and by Bagchi−Fleming−Oxtoby.[49] In each case, a nonradiative drain is assumed to couple S_1 and S_0 states, with the wave packet diffusing along the potential surface until reaching the drain. In the nonlocal sink models, k_{NR} is assumed to vary continuously with the torsional twist coordinate. These latter models were developed primarily to account for the viscosity-controlled ultrafast deactivation in triphenyl methane dyes where k_{NR} is at least 50-fold faster than for **ROBOD** in the same solvent. **ROBOD** does not conform to barrierless crossing, not least because of the relatively slow decay processes, even in low-viscosity solvents where there is a small barrier to reach the nonradiative drain. This situation can be treated in terms of Kramers' theory[50] for passage over a small barrier along a parabolic potential surface, although we cannot rule out the nonlocal pinhole sink model mentioned above,[48,49] and a more detailed analysis is required.

Concluding Remarks

This investigation has shown that sterically unhindered Bodipy dyes function as superior reporters for changes in local viscosity and/or polarizability. A clear advantage of such materials relative to all other available fluorescent probes concerns their facile derivitization and there is virtually no limit to the range of sensors that might be prepared. The absorption and emission maxima can be modified by well established protocols[15] and it is now possible to replace the fluorine atoms with ancillary photon collectors.[51] These dyes are resistant to intersystem crossing and are highly photostable. The precise mechanism by which **ROBOD** responds to changes in viscosity must await collection of more detailed experimental and theoretical data but our current understanding suffices to design improved sensors. A key point here is the structural distortion of the dipyrrin framework that accompanies rotation of the *meso*-phenyl ring. Our computational studies show that this deformation involves concerted buckling of the upper rim of the dipyrrin unit in the same plane (Figure 1). It should be possible to facilitate this geometry change by subtle modification at the boron atom, perhaps replacing boron with one of the several atoms known to coordinate to dipyrrin. This is the key feature by which to increase the sensitivity of the probe. Other desirable elements, including water solubility and attachment to proteins or inert substrates, are easily accomplished by standard synthetic methodologies.

We have shown also that important insight into the rheological properties of the surroundings can be obtained by the application of high pressures under isothermal conditions. This approach gives access to a very wide viscosity range without having to change the nature of the solvent. Dyes such as **ROBOD** can be used to record how certain fluids respond to changes in applied pressure by techniques that are much simpler than conventional viscosity measurements. Similar studies can be applied to biological membranes and microheterogeneous media, such as micelles, vesicles, and organo-gels.

Acknowledgment. We thank EPSRC (EP/E014062/1) and the University of Newcastle for financial support of this work. Drs. J. P. Rostron and V. Autissier are thanked for their help in setting up the high-pressure rig and M. Freeman is acknowledged for providing technical assistance with this instrument.

Supporting Information Available: Additional spectroscopy figures, plots, deconvoluted spectra, computed electron density maps, and NMR spectra for all new compounds (PDF). This material is available free of charge via the Internet at http://pubs.acs.org.

CM800702C

(46) Ben-Amotz, D.; Harris, C. B. *J. Chem. Phys.* **1987**, *86*, 4856–4870.
(47) Oster, G.; Nishijima, Y. *J. Am. Chem. Soc.* **1956**, *78*, 1581–1584.
(48) Förster, T.; Hoffmann, G. *Z. Phys. Chem N.F.* **1971**, *75*, 63–76.
(49) Bagchi, B.; Fleming, G. R.; Oxtoby, D. W. *J. Chem. Phys.* **1983**, *78*, 7375–7384.
(50) McCaskill, J. S.; Gilbert, R. G. *Chem. Phys.* **1979**, *44*, 389–402.
(51) Goze, C.; Ulrich, U.; Mallon, L. J.; Allen, B. D.; Harriman, A.; Ziessel, R. *J. Am. Chem. Soc.* **2006**, *128*, 10231–10239.